J|A|C|S COMMUNICATIONS

Published on Web 08/06/2009

Cross-Medal Arrays of Ta-Doped Rutile Titania

Xianfeng Yang,[†,‡] Jian Chen,[‡] Li Gong,[‡] Mingmei Wu,[‡] and Jimmy C. Yu*[,†]

Department of Chemistry and Centre of Novel Functional Molecules, The Chinese University of Hong Kong, Shatin, Hong Kong, China, and State Key Laboratory of Optoelectronic Materials and Technologies, School of Physics and Engineering, Instrumental Analysis and Research Centre, MOE Key Laboratory of Bioinorganic and Synthetic Chemistry, School of Chemistry and Chemical Engineering, Sun Yat-Sen (Zhongshan) University, Guangzhou 510275, China

Received May 28, 2009; E-mail: jimyu@cuhk.edu.hk

Morphological controlled growth of nano/microstructured crystals has attracted considerable attention because the properties of a material are strongly dependent on its structure.[1] A widely used approach for manipulating the crystal growth behavior in liquid systems is to employ appropriate capping reagents, e.g., organic surfactants or inorganic ions.[2] The capping reagents can preferentially adsorb on some specific crystallographic planes to block or retard their growth resulting anisotropic shape evolution process. The problem of this method is that the surface of the product would be covered by a passivation layer, which limits its practical use. As we know, the evolution of crystal architecture is always influenced by the intrinsic growth process related to the inner crystalline structures.[3] Recently, it has been demonstrated that the final morphologies of crystals could be tailored by doping ions into the crystal lattices to alter their growth patterns.[4] Metal-doped semiconductors, including Ta-doped TiO_2, have been widely studied for improved physical and chemical properties owning to the significant effects of the metal ion dopants on their inner electronic and/or crystalline structures.[5,6] In this communication, we demonstrate, for the first time, a facile Ta-doping induced hydrothermal growth route for the synthesis of rutile arrays consisting of cross-medal structures without using any capping reagents, seeds, or templates. Interestingly, the unusual epitaxial growth direction of the rutile cross-medal is determined by the orientation of the substrate.

The oriented rutile cross-medal arrays are assembled on a Tantalum foil which serves as both a substrate and doping source (see the Supporting Information for experimental details). Figure 1a shows a typical large-area view of the products (see Figure S1 in the Supporting Information for more details). Results from XRD and Raman analysis indicate that the as-synthesized sample is pure rutile phase (see Figures S2 and S3 in the Supporting Information). Viewing from the top of an individual crystal (Figure 1b), the arm of the cross is ~2.4 μm long with a diameter of ~440 nm. However, the three-dimensional morphology is more complex and interesting. From the continuous tilted observation (see video in the Supporting Information) and an enlarged side-view (Figure 1c), it can be clearly seen that almost all the as-prepared crystals stand vertically on the substrate. Each cross consists of two dumbbell-like bars perpendicular to each other. Together with the small nanoneedles formed around the center, the final architecture closely resembles a cross-medal (inset in Figure 1c).

TEM/HRTEM images and SAED pattern (Figure 1d and e) provide further insight into the microstructure and crystalline construction of the product. As shown in Figure 1d, this structure is single-crystalline in nature. All the measured distinct *d*-spacing values of 0.32 nm marked in the HRTEM image (Figure 1e) correspond to {110} lattice fringes of rutile titania with unit parameters $a = b = 0.459$ nm and $c = 0.296$ nm (JCPDS card 21−1276), consistent with the XRD analysis result (see Figure S2 in the Supporting Information). Furthermore, the single-crystalline SAED pattern and high resolution TEM image with related FFT pattern inset reveal that this crystal is projected along the [001] zone axis, and all the branches including main trunks and nanoneedles grow along the ⟨110⟩ directions. This is further confirmed by TEM and SAED measurements along the [110] zone axis (see Figures S4a, b in the Supporting Information). The rutile cross-medal contains ~3.6 mol % of tantalum as shown in the energy-dispersive X-ray (EDX) spectrum (see Figure S4c in the Supporting Information). Moreover, this novel Ta-doped rutile TiO_2 cross-medal array shows highly enhanced field-emission (FE) properties with a threshold field voltage of ~11 V/μm. This is much lower than the ~23 V/μm of rutile nanowire arrays reported before (see Figure S5 in the Supporting Information).[7]

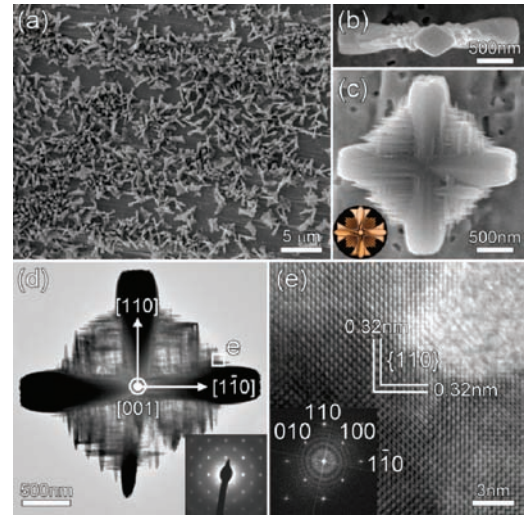

Figure 1. (a) Low-magnification SEM image of the as-prepared rutile cross-medal arrays grown at 180 °C for 6.0 h. (b) Top- and (c) side-view of a typical individual crystal; the inset of c is an image of a "Distinguished Flying Cross" medal of the U.S. Army. (d) TEM image of an individual crystal scratched from the substrate projected along the [001] zone axis with the related SAED pattern taken from the whole particle (inset). (e) HRTEM image comes from the corresponding square area e marked in (d) with the related FFT pattern (inset).

To decipher the growth mechanism, we investigated the morphological evolution of rutile cross-medal based on the time-dependent experiments (Figure 2 and Figure S6 in the Supporting Information). At the initial stage of 3.0 h, a sparse growth of cross-shaped rutile crystals on the Ta substrate was observed (see Figure S6a in the Supporting Information). Each crystal was composed of two main cross-linked trunks grown along ⟨110⟩ directions with diameters of ~200 nm and lengths of ~1.8 μm. Meanwhile, a few nanoneedles

[†] The Chinese University of Hong Kong.
[‡] Sun Yat-Sen (Zhongshan) University.

10.1021/ja904337x CCC: $40.75

began to show up (Figures 2a1−2). After 6.0 h of the reaction, denser rutile cross-medal array appeared on the substrate (Figure 1a). At 10 h, the parallel nanoneedles were more apparent and they fused together the mid main trunks. The terminated {110} facets look like a cross-section of a double-edged blade (Figure 2b1). Figures 2b3−6 show the typical high-angle annular dark field scanning TEM (HAADF-STEM) and EDX elemental mapping images of an individual crystal, further verifying the existence of Ta doped in the entire particle.

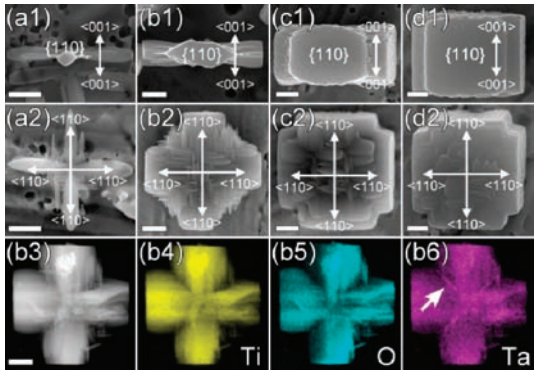

Figure 2. (a1−d1) Top- and (a2−d2) side-view of the sample a−d obtained at (a1, a2) 3.0, (b1, b2) 10, (c1, c2) 15, and (d1, d2) 20 h, respectively. (b3) HAADF-STEM and (b4−b6) elemental mapping images of an individual sample b (scale bar = 500 nm).

Because the ionic radii are about the same, Ta^{5+} can substitute for Ti^{4+} in the crystal lattice.[6] It is proposed that the surface energies of {110} planes would be increased higher than {001} planes in the presence of the dopant as previously observed in the $CaTiO_3$ systems.[4] Meanwhile, the crystalline lattice microstrains from the distortion of the $Ti(Ta)O_6$ octahedra along the *c*-axis would retard the growth along this direction. Therefore, the rutile prefers to grow along ⟨110⟩ instead of ⟨001⟩ directions to form cross-medal structures with a small aspect ratio of *c*/*a* much less than one. This is difficult to achieve otherwise because of the high surface energy of {001} planes.[8] Moreover, as indicated by an arrow in Figure 2b6, the dopant seems to concentrate in the grooves at the conjunctions, which would be the seed sites for nanoneedles branches grown along ⟨110⟩ directions. More detailed descriptions about the effects of Ta dopant on the growth patterns are given in Figure S7 of the Supporting Information.

It is well-known that the epitaxial and anisotropic nucleation and growth is strongly dependent on the atom arrangement at the nucleation sites.[9] Herein, the tantalum substrate has a cubic phase (JCPDS card 04−0788, $a = b = c = 0.3306$ nm) with a preferential orientation along ⟨100⟩ perpendicular to the surface as suggested by the XRD pattern (see Figure S2 in the Supporting Information).

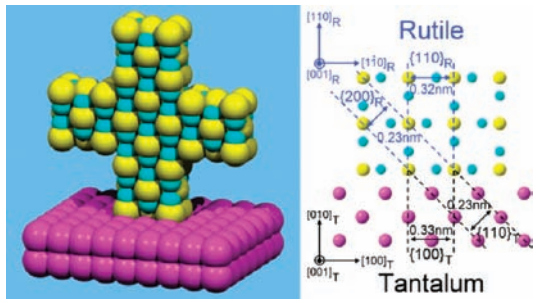

Figure 3. (Left) Schematic model of rutile cross medal grown from the tantalum substrate and (right) the related atomic arrangement comparison. The yellow, blue, and pink balls correspond to Ti(Ta), O, and Ta, respectively.

As shown in Figure 3, the lattice spacings of $\{200\}_R$ and $\{110\}_R$ in rutile are extremely close to those of $\{110\}_T$ and $\{100\}_T$ in tantalum. The ⟨110⟩ orientated and vertical epitaxial growth of rutile from the {100} plane of tantalum foil can therefore be attributed to the perfect match of their inner crystalline structures. A prolonged reaction time for 15−20 h would increase the thickness of the cross because of the growth along the *c*-axis as compared to the ⟨110⟩ directions (c1−2 and d1−2 in Figure 2). This is presumably due to the gradually diminishing free Ta ions in the reaction, and therefore Ostwald Ripening takes over as would be in a nondoped rutile system.

In conclusion, monodisperse rutile TiO_2 with cross-medal morphologies have been fabricated via a simple Ta-doping induced hydrothermal method. The structural characterization shows this rutile cross-medal has a unique growth behavior with a preferred orientation of ⟨110⟩ directions, which is very different from the *c*-axis of the traditional ones. Based on the preliminary results, this rutile cross-medal array exhibits efficient FE performance. This interesting branched TiO_2 with lowered band gap energy due to doping would be more active for photochemical reactions. Moreover, its single-crystalline nature is beneficial to the electron conduction in a photocatalytic system. Therefore, it can be expected that this TiO_2 material would have potential applications in dye-sensitized solar cells.

Acknowledgment. This work was supported financially by a Strategic Investments Scheme administrated by The Chinese University of Hong Kong and China Postdoctoral Science Foundation (20080440117) and NSFC (50872158).

Supporting Information Available: XRD patterns, Raman spectrum, and more SEM/TEM images with SAED pattern and EDX spectrum further show the structures of the as-prepared products. This material is available free of charge via the Internet at http://pubs.acs.org.

References

(1) (a) Lee, I.; Delbecq, F.; Morales, R.; Albiter, M. A.; Zaera, F. *Nat. Mater.* **2009**, *8*, 132. (b) Tsung, C. K.; Kuhn, J. N.; Huang, W. Y.; Aliaga, C.; Hung, L. I.; Somorjai, G. A.; Yang, P. D. *J. Am. Chem. Soc.* **2009**, *131*, 5816. (c) Li, H. X.; Bian, Z. F.; Zhu, J.; Zhang, D. Q.; Li, G. S.; Huo, Y. N.; Li, H.; Lu, Y. F. *J. Am. Chem. Soc.* **2007**, *129*, 8406.
(2) (a) Jun, Y. W.; Choi, J. S.; Cheon, J. *Angew. Chem., Int. Ed.* **2006**, *45*, 3414. (b) Yang, H. G.; Sun, C. H.; Qiao, S. Z.; Zou, J.; Liu, G.; Smith, S. C.; Cheng, H. M.; Lu, G. Q. *Nature* **2008**, *453*, 638. (c) Sounart, T. L.; Liu, J.; Voigt, J. A.; Hsu, J. W. P.; Spoerke, E. D.; Tian, Z.; Jiang, Y. B. *Adv. Funct. Mater.* **2006**, *16*, 335. (d) Yan, Q. Y.; Raghuveer, M. S.; Li, H. F.; Singh, B.; Kim, T.; Shima, M.; Bose, A.; Ramanath, G. *Adv. Mater.* **2007**, *19*, 4358.
(3) Ross, F. M. *Nat. Nanotechnol.* **2009**, *4*, 17.
(4) Alfredsson, M.; Cora, F.; Dobson, D. P.; Davy, J.; Brodholt, J. P.; Parker, S. C.; Price, G. D. *Surf. Sci.* **2007**, *601*, 4793.
(5) (a) Li, J.; Zeng, H. C. *J. Am. Chem. Soc.* **2007**, *129*, 15839. (b) Li, L.; Tsung, C. K.; Yang, Z.; Stucky, G. D.; Sun, L. D.; Wang, J. F.; Yan, C. H. *Adv. Mater.* **2008**, *20*, 903. (c) Bussian, D. A.; Crooker, S. A.; Yin, M.; Brynda, M.; Efros, A. L.; Klimov, V. I. *Nat. Mater.* **2009**, *8*, 35. (d) Yu, J. C.; Li, G. S.; Wang, X. C.; Hu, X. L.; Leung, C. W.; Zhang, Z. D. *Chem. Commun.* **2006**, 2717.
(6) (a) Pan, H. B.; Chen, N. S.; Shen, S. F.; Huang, J. L. *J. Sol−Gel Sci. Technol.* **2005**, *34*, 63. (b) Morgan, B. J.; Scanlon, D. O.; Watson, G. W. *J. Mater. Chem.* **2009**, *19*, 5175.
(7) Xiang, B.; Zhang, Y.; Wang, Z.; Luo, X. H.; Zhu, Y. W.; Zhang, H. Z.; Yu, D. P. *J. Phys. D: Appl. Phys.* **2005**, *38*, 1152.
(8) (a) Feng, X. J.; Zhai, J.; Jiang, L. *Angew. Chem., Int. Ed.* **2005**, *44*, 5115. (b) Yang, X. F.; Zhuang, J. L.; Li, X. Y.; Chen, D. H.; Ouyang, G. F.; Mao, Z. Q.; Han, Y. X.; He, Z. H.; Liang, C. L.; Wu, M. M.; Yu, J. C. *ACS Nano* **2009**, *3*, 1212. (c) Liu, B.; Aydil, E. S. *J. Am. Chem. Soc.* **2009**, *131*, 3985. (d) Barnard, A. S.; Curtiss, L. A. *Nano Lett.* **2005**, *5*, 1261.
(9) (a) Kuykendall, T.; Pauzauskie, P. J.; Zhang, Y. F.; Goldberger, J.; Sirbuly, D.; Denlinger, J.; Yang, P. D. *Nat. Mater.* **2004**, *3*, 524. (b) Yang, H. G.; Zeng, H. C. *J. Am. Chem. Soc.* **2005**, *127*, 270. (c) Zhang, D. F.; Sun, L. D.; Jia, C. J.; Yan, Z. G.; You, L. P.; Yan, C. H. *J. Am. Chem. Soc.* **2005**, *127*, 13492.

JA904337X